Whispering Gallery Mode Laser in an Elliptical Microring

Reyhan Baktur[1], L. W. Pearson[2], and J. M. Ballato[3]
[1] Department of Electrical and Computer Engineering
Utah State University, Logan, UT 84322, USA
breyhan@engineering.usu.edu

[2]Holcombe Department of Electrical and Computer Engineering
Clemson University, Clemson, SC 29634-0915
PL@exchange.clemson.edu

[3]Center for Optical Materials Science and Engineering Technologies (COMSET)
School of Material Science and Engineering
Clemson University, Clemson, SC 29634-0971
JBALLAT@exchange.clemson.edu

***Abstract*─** Studies on whispering gallery mode (WGM) laser in microrings have been limited to circular geometry. Elliptical microring lasers, despite their potential engineering use, have not been analyzed to guide experiments. This paper introduces a computationally efficient method for determining the WGM laser resonance and the laser field distribution in an elliptical microring. An analytical method is applied to avoid computing high order Mathieu functions. Both WGM resonant frequencies and electromagnetic (EM) field distributions are computed and presented in this paper. Computed results clearly show that the WGM laser field is concentrated on the outer surface of the microring. Results also show that the eccentricity of the ellipse affects the distribution of resonant frequencies and the laser field.

***Index Terms*─** Whispering gallery mode, microring laser, elliptical microring, Mathieu functions.

I. INTRODUCTION

The demonstration of lasers in luminescent conducting polymer thin films [1, 2] has triggered scientists to study lasers achieved with cylindrical microcavities formed with this type of polymer [3-6]. It is reported that a cylindrical microlaser based on whispering gallery mode (WGM) shows the advantages of supporting low-power operation and hence yields a high-Q value [3, 4]. The phenomenon of the whispering gallery was first observed and studied by Lord Rayleigh [7], and the electromagnetic (EM) WGM in a dielectric waveguide was comprehensively analyzed by Wait [8]. Considering the advantage of the low threshold lasing characteristics of microrings as well as the flexibility of forming the conjugate polymer into various geometry [2], there is a potential engineering use of microring lasers as integrated signal sources for communications. Experimental measurements on the lasing spectrum of polymer cylindrical microlasers have been reported [4], and simplified studies for resonant modes were presented by several researchers [5, 6]. Baktur et. al. provided a more comprehensive theoretical description for WGM laser resonances in a circular microring [9].

While microring geometry has been confined to a circular cross-section so far, it is equally important to study the WGM laser in an elliptical microring because such a structure provides a controllable coupling when used as a pump source. It is the objective of this work to develop a computationally efficient method for determining the resonance and fields of a WGM laser in a microring with an elliptical cross-section. The paper is organized as follows. Section II describes the problem solving method and basic formula in an elliptical geometry. Computation, results, and discussions of WGM resonance and fields are presented in sections III and IV. Limiting factors of the method are concluded in section V.

II. CONFIGURATION OF THE LASER

The configuration of the elliptical microring is as follows. A microring made from an optically active polymer is built on an aluminum or gold core. Both core and ring are of elliptical cross-section (see Fig. 1). The choice of the core material is consistent with the experimental studies [3, 4]. Although waveguide modes exist and can resonate in a microring, to be consistent with experiments [3, 4], we only discuss modes that are detached from the inner boundary of the microring, i.e. WGMs. The microring is modeled to have an infinite length (i.e. infinite in z. It should be noted that Fig. 1 is on xy plane, and z is vertical to the cross section in xy plane.) because the optical length of the microring is in the order of 100 wavelengths and allows us to model the length as infinite for the simplicity of the analysis. The microring can, of course, support propagation in the z direction, bounded by reflections on the annular faces. However, such a mode structure involves radiative loss at these interfaces, and the losses would quench lasing.

The cross-section view of the microring is shown in Fig. 1. Major and minor axes of the inner boundary of the microring are denoted as a, b. For the outer boundary, the two axes are a' and b'. The thickness of the microring is d, and it is obvious to see that the following relations hold,

$$a' = a + d,\quad b' = b + d. \tag{1}$$

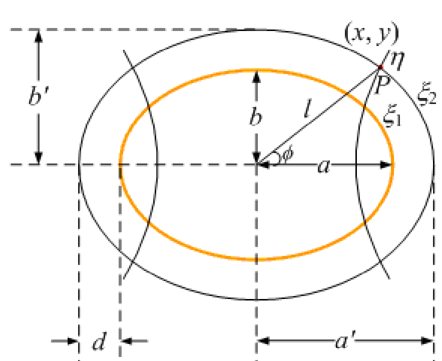

Fig. 1. Cross-section view of the elliptical microring.

In elliptical coordinates, the two-dimensional wave equation can be separated into two Mathieu's equations [11, 12], and solutions of these two equations are combinations of Mathieu's functions [13]. Since WGMs are high order modes [7, 8], it suggests that in order to study the WGM in an elliptical microring, we need to deal with modes involving Mathieu functions of large orders. Although it is possible to study the WGM resonance in an elliptical cavity by evaluating Mathieu functions [14], the mode numbers that can be correctly computed are rather limited. Summations for Mathieu functions of large orders are difficult due to their poor convergence. Additionally, the process of deriving formula for EM field components is very tedious and time consuming. Therefore, we try to provide a much simpler formulation with a smaller computational complexity.

Before computing the WGM resonance and electromagnetic fields, it is helpful to work out relations between variables used in the elliptical coordinate system. In Fig. 1, a point p on the outer ellipse can be located by any one pair of variables from (x, y), (l, ϕ) or (ξ_2, η). The relations between these three sets of variables are as follows:

$$x = l\cos\phi,\quad y = l\sin\phi, \tag{2}$$

$$x = a'\cos\eta,\quad y = b'\sin\eta, \tag{3}$$

$$l = \sqrt{x^2 + y^2},\quad \cos\phi = \pm\frac{a'}{l}\sqrt{\frac{l^2 - b'^2}{a'^2 - b'^2}}, \tag{4}$$

$$\cos\eta = \frac{l}{a'}\cos\phi,\quad \sin\eta = \frac{l}{b'}\sin\phi, \tag{5}$$

and

$$\tanh\xi_2 = \frac{b'}{a'}. \tag{6}$$

The method proposed to study the WGM laser in an elliptical microring is to deduce the WGM field from the propagation in a local osculating circle [15]. This method has been validated with experiments for WGM in an elliptical microdisk

[15]. At a point in the microring, the laser field is approximated by the field in the circle of curvature at that point.

To begin the discussion, the outer ellipse (axes: a', b') is fit locally with circles of curvature as illustrated in Fig. 2. For example, at the point P on the ellipse (axes: a', b'), the circle of curvature is C_1. C_1 is an osculating circle at P, and it has the same radius as the radius of curvature at the point P. The radius of curvature at a point (ξ_2, η), represented by $R(\eta)$, can be computed from the following formula [16]:

$$R(\eta) = \frac{(a'^2 \sin^2\eta + b'^2 \cos^2\eta)^{\frac{3}{2}}}{a'b'}. \tag{7}$$

The WGM field at P_1 in the ellipse is viewed as having the same property as the WGM field at P_1 in the circle C_1. Therefore, computing the field at P_1 in C_1 approximates the field in the ellipse at P_1. Similarly, fields at P_2 and P_3 can be obtained by computing fields in the circle C_2 and C_3 at these points. When circles of curvature are fit into the ellipse at every point, the field at any point inside the ellipse (i.e. P_1 and P_3 Fig. 2) and outside the ellipse (i.e. P_2 in Fig. 2) can be accordingly computed.

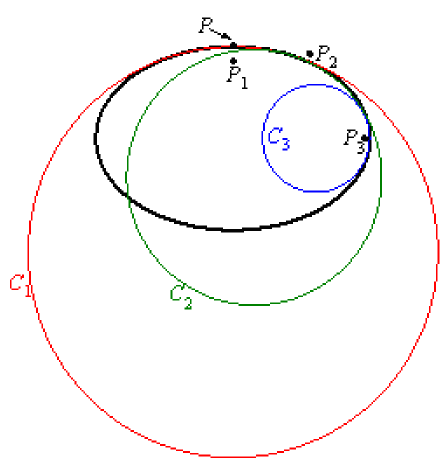

Fig. 2. Ellipse with its osculating circles at three points.

III. WHISPERING GALLERY MODE RESONANCE

A. Analysis

When computing the resonance, the EM fields are separated into transverse electric (TE) and transverse magnetic (TM) modes to z axis, which is along the length of the microring. The two types of modes are then treated individually. In the local circle (i.e. the circle of curvature), the circumferential propagation is contained in $e^{-j\nu\phi}$, where ν is the angular wave number [9], and ϕ is the angular distance on the local circle. It is desirable to rewrite $e^{-j\nu\phi}$ into $e^{-j\nu(\eta)\phi(\eta)}$ to show local propagation. When a WGM propagates along the ellipse, for a whole period, the increase in phase along the path of the angular propagation is $\int_{\eta=0}^{\eta=2\pi} \nu(\eta)\phi(\eta)d\eta$. In order to achieve a WGM resonance the phase increase needs to be an integer multiple of 2π when the EM wave finishes an entire period along the ellipse. Accordingly we have equation (8), where m is an integer and $\nu(\eta)$, which is closely related to the radius of the curvature [9], is the order of the Bessel functions that describe the WGM in the local microring at η.

$$\int_{\eta=0}^{\eta=2\pi} \nu(\eta)\phi(\eta)d\eta = 2m\pi. \tag{8}$$

In equation (8), $\phi(\eta)$ is the angular distance along the local circle at η and the corresponding length on the local circle is

$$l(\eta) = R(\eta)\phi(\eta). \tag{9}$$

It should be noted that at the vicinity of (ξ, η), $l(\eta)$ can be approximated by the arc-length of the ellipse along $d\eta$ and it yields

$$l(\eta) = \sqrt{a'^2 \sin^2\eta + b'^2 \cos^2\eta}\, d\eta. \tag{10}$$

Using (7), (9) and (10), (8) can be re-written into

$$\int_0^{2\pi} \frac{a'b'}{a'^2 \sin^2\eta + b'^2 \cos^2\eta} \nu(\eta)d\eta = 2m\pi. \tag{11}$$

When the ellipse takes the limit to a circle, (11) gives $\nu = m$. This result is the same as discussed in [9] for a circular microring resonance. By using a zero finding routine, $\nu(\eta)$ can be computed from the characteristic equation of the local microring.

B. Computed Results

Resonant frequencies (wavelengths) for both TM and TE WGM modes in elliptical microrings are computed and the results are plotted in Fig. 3. The elliptical microrings have the same perimeters and have varied axial ratios. In computation, the integration in equation (11) is divided into 80 sub-intervals, and the Gaussian quadrature with the order of 32 is used over sub-intervals. From Fig. 3, it is seen that the axial ratio of the ellipse affects the resonance by shifting the resonant wavelengths. But the shifting is not significant when the laser resonance (630 *nm*) is considered. Also, the spacing between the wavelengths does not change significantly according to the shape of the ellipse as long as the perimeter of the ellipse stays the same.

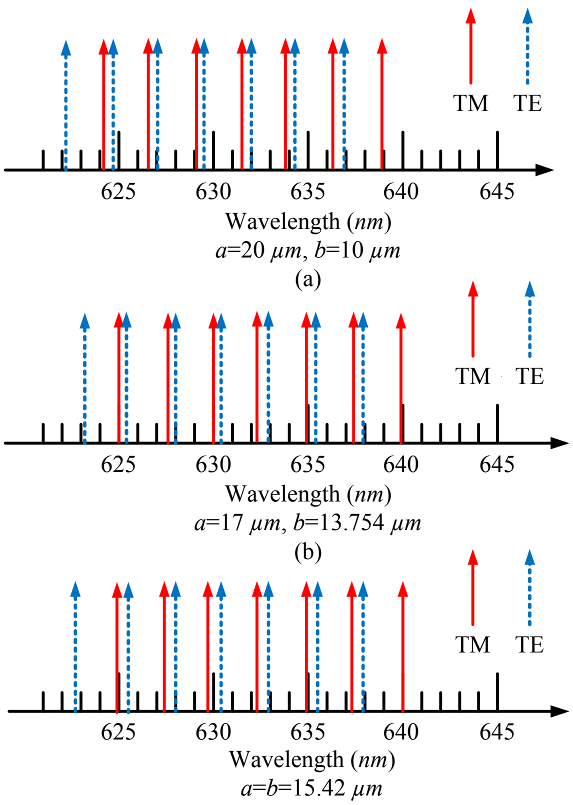

Fig. 3. WGM resonance in an elliptical microring with respect to the axial ratio.

C. Discussion

It is useful to have a simplified formula to approximately determine the resonant wavelengths to guide experiments. Suppose at λ_0 there is a WGM resonance, then equation (8) holds for λ_0, and it means the equation (12) shown below is true. The refractive index of the microring is n_r.

$$\frac{2\pi n_r}{\lambda_0}\int_0^{2\pi}\frac{\lambda_0}{2\pi n_r}\frac{ab}{a^2\sin^2\eta+b^2\cos^2\eta}\nu(\eta)d\eta = 2\pi m\,. \tag{12}$$

If we let $L=\int_0^{2\pi}\frac{\lambda_0}{2\pi n_r}\frac{ab}{a^2\sin^2\eta+b^2\cos^2\eta}\nu(\eta)d\eta$,

Since $\nu(\eta)$ is related to $R(\eta)$ [8], $\nu(\eta)$ can be rewritten as

$$\nu(\eta)=\frac{2\pi}{\lambda_0}n_r\alpha(\eta)R(\eta), \tag{13}$$

where $\alpha(\eta)$ is a coefficient. So L becomes

$$\begin{aligned} L &= \int_0^{2\pi}\alpha(\eta)\frac{ab}{a^2\sin^2\eta+b^2\cos^2\eta}R(\eta)d\eta \\ &= \int_0^{2\pi}\alpha(\eta)\sqrt{a^2\sin^2\eta+b^2\cos^2\eta}\,d\eta\,. \end{aligned} \tag{14}$$

Therefore, from (12), we have

$$L(n_r/\lambda_0)=m\,. \tag{15}$$

Suppose that a new resonance occurs at $\lambda_0+\Delta\lambda$ and results in an integer m-1 for (15). L varies slowly compared to $\Delta\lambda$, and one can assume that L does not change with respect to the wavelength. Therefore, we have

$$\frac{n_r}{\lambda_0+\Delta\lambda}L\approx m-1. \tag{16}$$

From (16), $\Delta\lambda$ can be computed as the following

$$\Delta\lambda\approx\frac{\lambda_0^{\,2}}{n_r\int_0^{2\pi}\alpha(\eta)\sqrt{a^2\sin^2\eta+b^2\cos^2\eta}\,d\eta}\,. \tag{17}$$

If we further assume $\alpha(\eta)\approx 1$, then $\Delta\lambda$ can be approximately computed from

$$\Delta\lambda\approx\frac{\lambda_0^{\,2}}{n_r\int_0^{2\pi}\sqrt{a^2\sin^2\eta+b^2\cos^2\eta}\,d\eta}\,. \tag{18}$$

Equation (18) is easy to compute and it gives a simple approximate check for experimental data, but it is an approximation because α approaches 1 only when the structure is electrically large. For example, it is found that α increased from 0.94 to 0.97 as the radius of curvature increased from 10.0 to 23.0 μm for the free space wavelength of 632.00 *nm*.

IV. COMPUTATION OF THE WGM FIELD

A. Analysis

When an excitation is placed near P_0 in the osculating circle C_0 (Fig. 4), the WGM field at P_0 can be determined from the radius of C_0 and ν_0, which is the order of the WGM. The EM field at P_1, which is located next to P_0, is on the osculating circle C_1. When P_0 and P_1 are in the vicinity of each other, both of them can be approximately viewed as in the circle C_1, and accordingly satisfy the following:

$$F(P_1) = F(P_0)e^{j\nu_1\Delta\phi}. \quad (19)$$

The exponent in (19) can be re-written to have

$$j\nu_1\Delta\phi = j\frac{\nu_1}{R_1}R_1\Delta\phi = j\frac{\nu_1}{R_1}\Delta l. \quad (20)$$

The arc-length can be computed from

$$\Delta l = \sqrt{a^2\sin^2\eta_1 + b^2\cos^2\eta_1}\,\Delta\eta, \quad (21)$$

where $\Delta\eta$ is the angular variation from P_0 to P_1 along the ellipse e, η_1 is the angular coordinate of P_1 on the ellipse e and the relation between η and ϕ is given by equation (5) .

By using (21), (20) becomes

$$j\nu_1\Delta\phi = j\frac{ab\nu_1}{a^2\sin^2\eta_1 + b^2\cos^2\eta_1}\Delta\eta. \quad (22)$$

Let $\Gamma_1 = \dfrac{ab\nu_1}{a^2\sin^2\eta_1 + b^2\cos^2\eta_1}$, and the equation (19) becomes

$$F(P_1) = F(P_0)e^{j\Gamma_1\Delta\eta}. \quad (23)$$

Similarly, fields at P_2 and P_3 can be computed from

$$F(\mathrm{P}_2) = F(P_1)e^{j\Gamma_2\Delta\eta} = F(P_0)e^{j\Gamma_1\Delta\eta}e^{j\Gamma_2\Delta\eta} = F(P_0)e^{j(\Gamma_1+\Gamma_2)\Delta\eta}, \quad (24)$$

and

$$F(P_3) = F(P_0)e^{j(\Gamma_1+\Gamma_2+\Gamma_3)\Delta\eta}. \quad (25)$$

Iterating this process gives the field at P_N to be

$$F(\eta) = F(P_0)\exp(j\sum_{i=1}^{N}\Gamma_i\Delta\eta). \quad (26)$$

When N approaches infinity, (26) becomes

$$F(\eta) = F(P_0)\exp[j\int_{\eta_0}^{\eta}\Gamma(\eta)d\eta]. \quad (27)$$

In order to have (27) valid for every η, a definition for Γ at η_0 is added to have

$$\Gamma(\eta) = \begin{cases} 0 & , \quad \eta = \eta_0 \\ \dfrac{ab\nu(\eta)}{a^2\sin^2\eta + b^2\cos^2\eta} & , \text{ otherwise.} \end{cases} \quad (28)$$

So, to compute a WGM field component at a general point P_η^r, we find the projection of P_η^r on the ellipse e, and denote the projection as (ξ_0, η). The distance from P_η^r to the ellipse is d_r. Then, on the ellipse with two axes ($a+d_r$, $b+d_r$), we locate a point P_0^r that can also be defined by the osculating circle C_0 and the distance d_r. For example, in Fig. 4, P_0^r is at (R_0+d, $\pi/2$), R_0 is the radius of C_0. The electromagnetic field at P_0^r can be computed from WGM field in a circular resonator as described in [17], and the EM field at P_η^r can be determined from

$$F(\mathrm{P}_\eta^r) = F(\mathrm{P}_0^r)\exp[j\int_{\eta_0}^{\eta}\Gamma(\eta)d\eta]. \quad (29)$$

It is important to make sure the correct η is used. In (29), η is associated with the outer ellipses e, and it can be determined from (3) or (5).

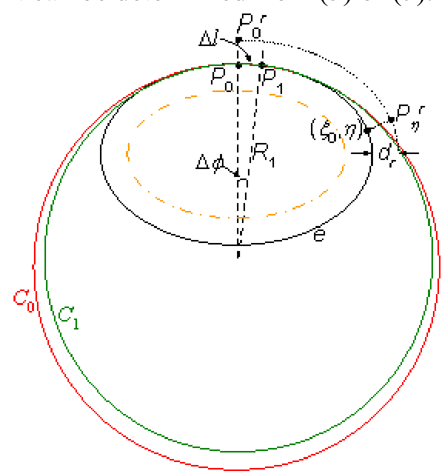

Fig. 4. Illustration of the elliptical microring with osculating circles.

B. Computational Considerations

The EM WGM field is studied by computing six field components (E_z, E_ρ, E_ϕ and H_z, H_ρ, H_ϕ). The z components are along length of the microring, and the other two components are along the radial and azimuthal axes of the elliptical cross section. To use the relation in (29) to compute EM field at the point P_η^r, the distance from this point to the outer ellipse and η is needed. It is simpler if the problem is discussed in the rectangular coordinate system. Suppose P_η^r is at (x, y), and we need to find its projection (ξ_0, η), which can be also located by (x_p, y_p). The distance between P_η^r and (ξ_0, η) satisfies

$$d_r(x_p, y_p)^2 = (x_p - x)^2 + (y_p - y)^2. \quad (30)$$

The projection of P_η^r is on the outer ellipse, so it satisfies

$$x_p^2 / a^2 + y_p^2 / b^2 = 1. \tag{31}$$

By making use of equation (31), d_r^2 can be converted to a function of only x_p or y_p. In order for (x_p, y_p) to be the projection of P_η^r, d_r^2 has to be the minimum value. So by searching for the zero around (x, y) of the $d(d_r^2)/dx_p$ or $d(d_r^2)/dy_p$, x_p and y_p can be located and η can then be found from either $\cos\eta = x_p / a$ or $\sin\eta = y_p / b$.

C. Computed Results

A WGM field excited by an infinite electric line source along the length of a microring is computed. The perimeter of the microring is fixed at 36π μm, and the axial ratio is varied from 1 to 2:1. The thickness of the microring is 4 μm. The source is located inside the microring on $\eta=\pi/2$, and it is 4.0 μm away from the outer boundary of the microring. The operation wavelength is chosen to be at λ=630.0 nm in free space. Magnitudes of the E_z component (i.e. $|E_z| = \sqrt{\mathrm{Re}(E_z)^2 + \mathrm{Im}(E_z)^2}$) in a microring with an axial ratio 1:1.5 is plotted in Fig. 5.

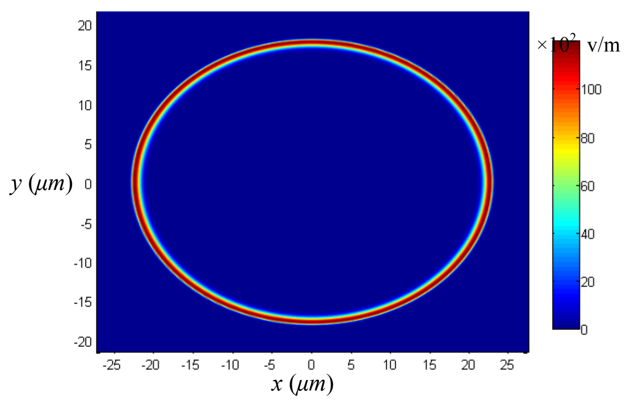

Fig. 5. Magnitude of E_z (v/m) when a:b=1.5.

It is clearly seen that the electromagnetic field concentrates at the outer boundary of the microring. From the figure the field decayed to 0 within less than 2.0 μm from the outer boundary, and the thickness of the ring is 4 μm. In order to see details of the WGM field, the real and imaginary parts of E_z are plotted along different ϕ as shown in Fig. 6- Fig. 8. Note that when $\phi=\pi/2$, it is the same ϕ plane where the source lies.

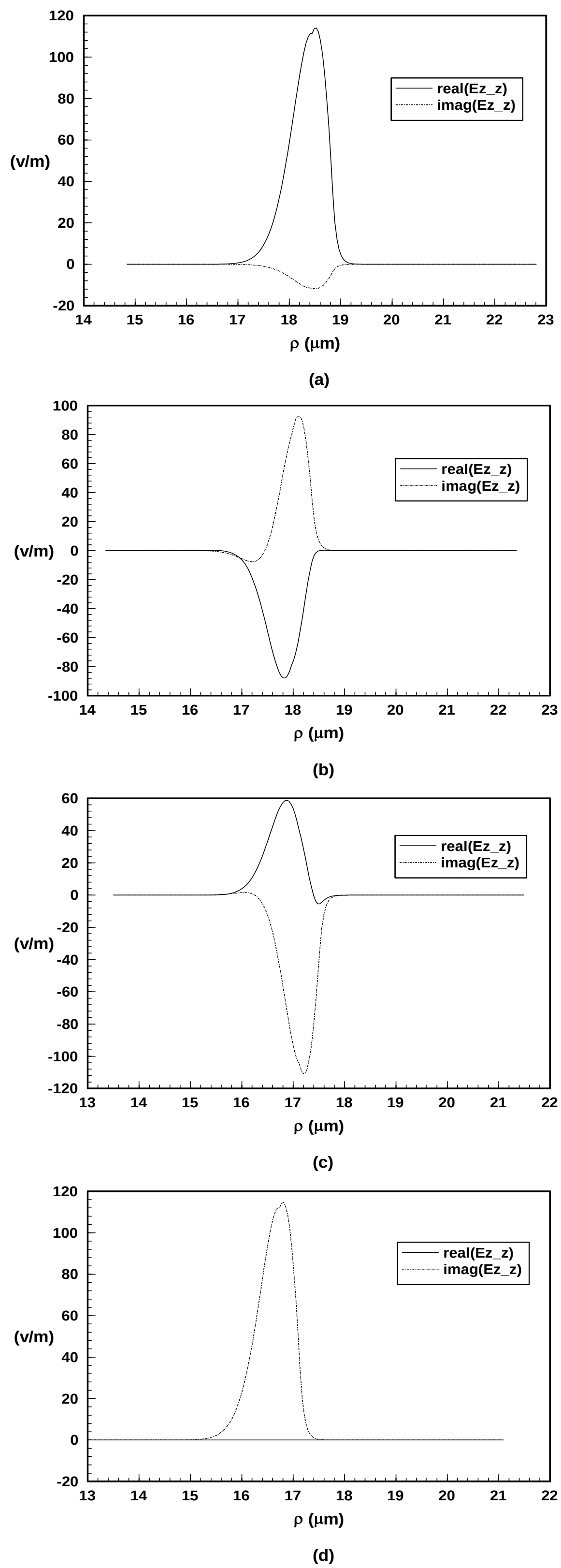

Fig. 6. Real and imaginary parts of E_z for a:b=1.1, ϕ=0, π/6, π/3 and π/2 respectively in (a) to (d).

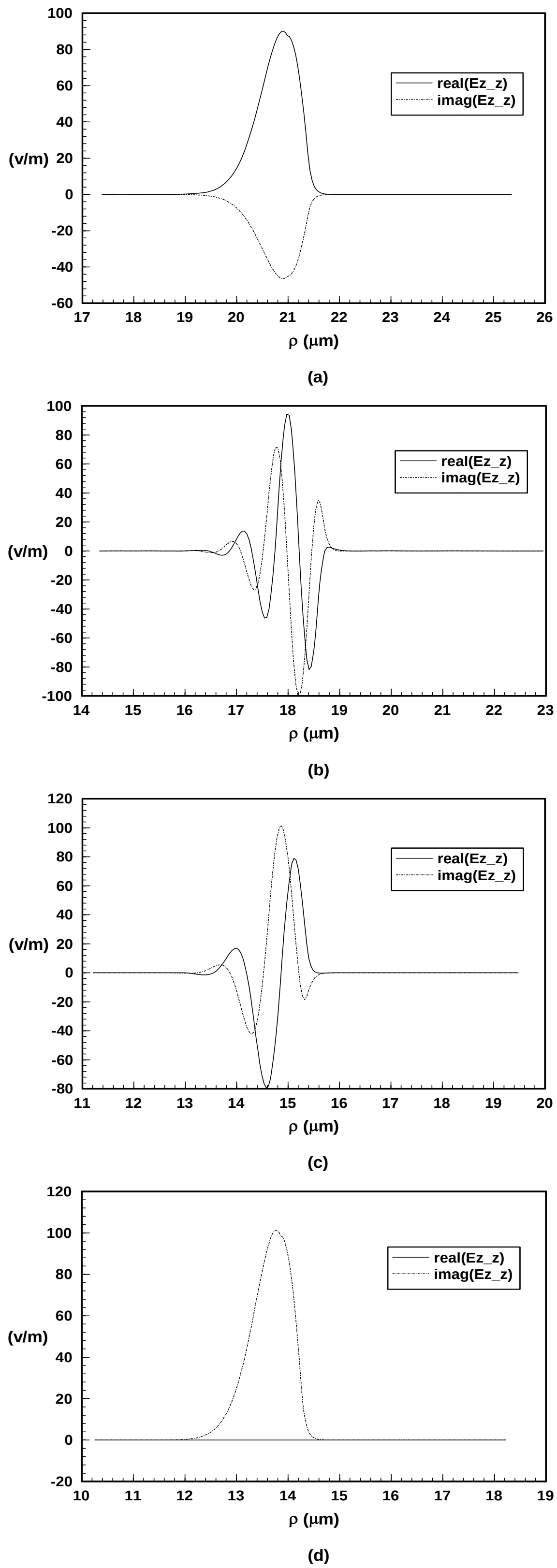

Fig. 7. Real and imaginary parts of E_z for a:b=1.5, ϕ=0, π/6, π/3 and π/2 respectively in (a) to (d).

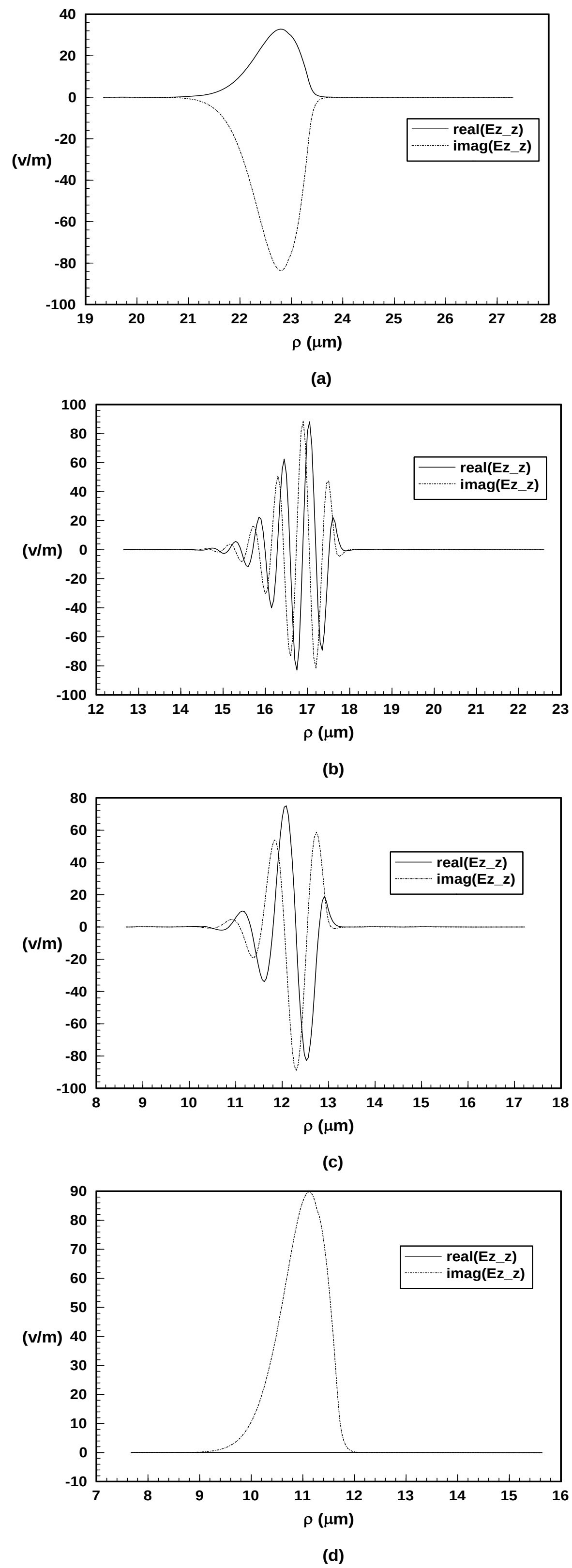

Fig. 8. Real and imaginary parts of E_z for a:b=2, ϕ=0, π/6, π/3 and π/2 respectively in (a) to (d).

D. Discussion

From section III, it is seen that the eccentricity of the ellipse affects the resonance by shifting the resonant frequency. Therefore when the axial ratio of the microring is changed, the excitation frequency needs to be shifted simultaneously to achieve a resonance. Otherwise, if the frequency is fixed to resonate for the circular microring, then as the microring becomes more eccentric, the excitation frequency is further away from the resonance, and it results in the decreased intensity of the EM field.

From Fig. 6 to Fig. 8, especially (c) and (d) of these figures, the phase of E_z changes along the constant ϕ line. This change can be understood with the illustration shown in Fig. 9, where the field at point P_1 has same phase as fields at points on l. P_s is the source point. Fields at these points are computed from WGM in the osculating circle of the outer ellipse at P_2'. The data are plotted along a constant ϕ while P_1 and P_2 are not both on the line l, and they are not computed from the same osculating circle. Therefore, P_1 and P_2 do not have the same phase unless when ϕ=$k\pi$ or ϕ=$k\pi$+π/2, where k is an integer.

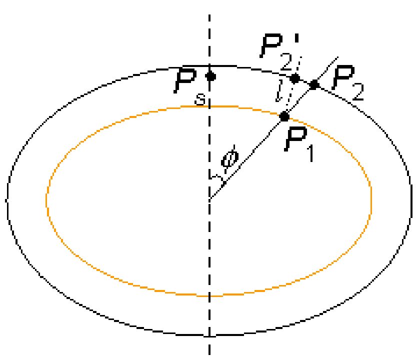

Fig. 9. Illustration of the phase plane of the WGM field in the elliptical microring.

V. CONCLUSION

For an elliptical microring, both WGM resonance and field components are computed by fitting the ellipse with circle of curvature. In computations, the assumption is made such that the WGM field at a point in the elliptical microring is the same as the WGM field in the circle of the curvature of the ellipse at that point. This assumption is valid for an electrically large elliptical microring where the electric radius of the microring is of the order of 100.

It is found that a change in the axial ratio of the elliptical microring results in a shift in the WGM resonant frequencies. Because the eccentricity shifts the resonance, when using the same excitation where a circular microring reaches its resonance, and then deforming the circular ring into an elliptical ring, it gives decreased magnitude of the laser field.

The method applied is valid for electrically large structures and therefore for the case of a highly eccentric ellipse. At the ends of the major axis, the circle of curvature may have a small radius, which may not support a WGM, and the method discussed will no longer be valid for such geometry.

One needs to pay attention to the thickness of the microring. As discussed in [9], the thickness of the ring to support the WGM is associated with the dimension of the structure. The bigger the radius of the microring, the thicker the microring must be. This means that for an elliptical microring, it has to be thick enough to support WGM at two ends of the minor axis (For example, P_0 in Fig. 4) because the osculating circle has the largest radius at this point. On the other hand, when a relatively thick circular microring is deformed into an elliptical microring, there may be a sharp edge at the major axis at the inner boundary and it may affect the computation and validity of the method presented.

REFERENCES

[1] N. Tessler, G. J. Denton and R. H. Friend, “Lasing of Conjugated Polymer Microcavities”, *Nature*, vol. 382, pp. 695-697, 1996.

[2] C. Kallinger, *et. al.*, “A Flexible Conjugated Polymer Laser”, *Adv. Mater.*, vol. 10, no.12, pp. 920-923, 1998.

[3] S. V. Frolov, A. Fujii, D. Chinn, Z. V. Vardeny, K. Yoshino, and R. V. Gregory, “Cylindrical Microlasers and Light-emitting Devices from Conducting Polymers”, *Appl. Phys. Lett.*, vol. 72, no. 2, pp. 2811-2813, 1998.

[4] S. V. Frolov, M. Shkunov, A. Fujii, K. Yoshino, and Z. V. Vardeney, “Lasing and Stimulated Emission in π–Conjugated Polymers”, *IEEE J. Quantum Elect.*, vol. 36, no. 1, pp. 2-11, 2000.

[5] R. C. Polson, G. Levina, and Z. V. Vardeny, "Mode Characterization of Microring Polymer Laser", *Synthetic Metals*, vol. 111, pp. 363-367, 2001.

[6] N. C. Frateschi and A. F. J. Levi, "Resonant Modes and Laser Spectrum of Microdisk Lasers", *Appl. Phys. Lett.*, vol. 66, no. 2, pp. 2932-2934, 1995.

[7] J. W. Strutt, "The Problem of the Whispering Gallery", *Philosophical Magazine*, vol. xx, pp. 1001-1004, 1910.

[8] J. R. Wait, "Electromagnetic Whispering Gallery Modes in a Dielectric Rod", *Radio Science*, vol. 2, no. 9, pp. 1005-1017, 1967.

[9] R. Baktur, L. W. Pearson and J. M. Ballato, "Theoretical Determination of Lasing Resonances in a Microring", *J. of Appl. Phys.*, vol. 101, no. 4, pp. 043102-043102, 2007.

[10] M. Abramowitz and I. A. Stegun, *Handbook of Mathematical Functions with Formulas, Graphs, and Mathematical Tables*, John Wiley & Sons, 1972.

[11] C. Yeh, "Elliptical Dielectric Waveguides", *J. Appl. Phys.*, vol. 33, no.11, pp. 3235-3243, 1962.

[12] L. A. Lyubimov, G. I. Veselov, and N. A. Bei, "Dielectric Waveguides with Elliptical Cross Section", *Radio Eng. Electron*. (USSR), vol. 6, pp. 1668-1677, 1961.

[13] N. W. McLachlan, *Theory and Application of Mathieu Functions*. Oxford, England: University Press, 1951.

[14] M. Matsubara, Y. Tomabechi, and K. Matsumura, "An Analysis for Resonance Characteristics of Whispering Gallery Modes on an Elliptic Dielectric Disk", *Proceedings of APMC, Taipei Taiwan,* pp. 473-475, 2001.

[15] Y. Kogami, Y. Tomabechi, and K. Matsumura, "Resonance Characteristics of Whispering-Gallery Modes in an Elliptic Dielectric Disk Resonator", *IEEE Tran. Microw. Theory Tech.*, vol. 44, no. 3, pp. 473-475, 1996.

[16] C. E. Pearson, *Handbook of Applied Mathematics*, Van Nostrand Reinhold Company, 1974.

[17] R. Baktur, L. W. Pearson, and J. M. Ballato, "Computation of Electromagnetic Whispering Gallery Mode Field in a Dielectric Microring Fabricated on a Metal Wire", *Electromagnetics*, vol. 29, no.1, pp. 1-12 , 2009.

Reyhan Baktur graduated from Clemson University in 2005 with a doctoral degree in electrical engineering, where she studied the whispering gallery mode laser in polymer microrings. She is currently an Assistant Professor of Electrical and Computer Engineering at Utah State University. Dr. Baktur is a member of IEEE.

L. Wilson Pearson is a Samuel R. Rhodes Professor of Electrical and Computer Engineering at Clemson University. His research interests include antennas, RF systems, and software-defined radio. Application areas include communications, spatial power combining, and low-cost phased-array antennas. Professor Pearson is an IEEE fellow and has served as Editor-in-Chief for the IEEE Transactions on Antennas and Propagation and on the Editorial Board of the IEEE Proceedings. He currently is Chair of USNC-URSI Commission D. He is a recipient of an IEEE Third Millennium Medal, the Provost's Award for Scholarly Excellence (Clemson University), and the McQueen Quattlebaum Faculty Achievement Award.

John Ballato is a Professor of Materials Science and Engineering at Clemson University where he also serves as Director of the Center for Optical Materials Science and Engineering Technologies (COMSET). He received his B.S. and Ph.D. degrees in Ceramic and Materials Science and Engineering from Rutgers. He has published over 160 archival papers with over 1500 citations, holds 25 US and foreign patents, and has given over 120 invited lectures and colloquia.